Supplementary Information for

Integrating wind into China's coal-heavy electricity system

Davidson, Michael R.[a,§], Zhang, Da[a,b,§], Xiong, Weiming[b],

Zhang, Xiliang[b], Karplus, Valerie J.[a,c,*]

Affiliations:

[a]China Energy and Climate Project, Joint Program on the Science and Policy of Global Change, Massachusetts Institute of Technology.

[b]China Energy and Climate Project, Institute of Energy, Environment, and Economy, Tsinghua University.

[c]Sloan School of Management, Massachusetts Institute of Technology.

[§]Michael Davidson and Da Zhang contributed equally to this work.

[*]To whom correspondence should be addressed. E-mail: vkarplus@mit.edu

This is a pre-publication version. For final version, see: https://doi.org/10.1038/nenergy.2016.86.

Please cite as:

Davidson, M. R., Zhang, D., Xiong, W., Zhang, X., & Karplus, V. J. (2016). Modelling the potential for wind energy integration on China's coal-heavy electricity grid. *Nature Energy*, *1*, 16086. https://doi.org/10.1038/nenergy.2016.86

This PDF file includes:

Materials and Methods:

Supplementary Text:

5. Full results
6. Validation of model representation of curtailment
7. Calculating non-fossil energy in 2030
8. Supply curve comparison

Materials and Methods

Here we describe the steps in our approach to estimating grid-integrated economic wind potential (Section 1-3) and an extensive set of sensitivity cases (Section 4) to evaluate the relationship between key integration parameters and simulated curtailment.

1. Physical resource characterization

1.1 Geographic exclusions

In this analysis, certain terrains (slopes greater than 10% and elevations greater than 5,000 meters), geographic features (forests, protected areas, lakes, and rivers), and built-up areas (major urban areas, industrial and transportation facilities) were not considered available for turbine siting. Offshore wind farms to date in China have been constructed in intertidal zones or water less than 20 meters deep. Fifty meters is seen as economically viable, and 100 meters is frequently used as a "deep sea" threshold[1].

1.2 Turbine spacing

Recent studies have reopened the debate on previous rules of thumb such as 3-5 rotor diameter spacing cross-wind and 5-9 diameter spacing down-wind in response to experimentally observed power fall-off at turbine spacings of up to 10 rotor diameters[2].

Onshore wind: Using a 1.5-MW Sinovel SL1500 turbine at 82-meter hub height, based on a survey of twelve existing wind farms in China, we find turbine spacing density ranging from 1.5MW-4.5MW/km^2. We assume 2.58 MW/km^2 for the base case spacing, or roughly 9×9 rotor diameter spacing.

Table S1. Turbine spacing density for 12 existing wind farms in China

Wind Farm	Spacing density (MW/km^2)
Bayin[*]	1.64
Wulan_No. 1[†]	3.71
Kangbao_Guodian[‡]	1.67
Beiqinghe[§]	2.54
Yihe_Huaneng	3
Yihe_Shenneng	3
Jieji_No. 1	2.97
Jianhua_No. 1	2.80
Jianhua_No. 2	2.67
Taipingzhao[#]	1.85
Fubei[‖]	1.5
Baotou[**]	4.5

Offshore wind: Using a 5-MW Sinovel SL5000 at 120-meter hub height offshore wind turbine, based on investigation of three existing and planning offshore project in China, we find the turbine spacing density ranges from 4.5-5.6MW/km^2. We assume 5 MW/km^2 for base case spacing.

Table S2. Turbine spacing density for offshore wind farms in China

Wind Farm	Spacing density (MW/km^2)
Zhoushan[††]	5
Pingtan[‡‡]	5.6
Jiaxing[§§]	4.5

Power curves for the turbines were obtained from the manufacturer (http://www.sinovel.com/).

2. Wind supply curve construction

2.1 Overview of the Routine

We construct a supply curve for wind at the national level using the procedure summarized in Figure S1. Our basic approach is to search for grid cells that allow integration at least cost across six regional combinations of wind origin and point of integration. We begin by calculating wind electricity generation costs per kilowatt-hour (kWh) for origin cells in the four regions (Northeast, Northwest, Sanhua, and South, as shown in Step (1) on the upper left in Figure S1). Generation cost (GenCost) is calculated using the NPV method described in SI 2.2, and added to integration within regions (i.e., no inter-regional transmission) for the first four options.

Costs associated with cross-regional transmission (available for Northeast-Sanhua and Northwest-Sanhua) are then calculated. These costs include the UHV transmission cost per kWh delivered (TransCost), calculated according to the average expected loading of the transmission line using the method described in SI 3.2.4. They also include the cost of curtailment due to congestion on the UHV transmission network (TransCurtCost, if relevant), calculated in the same fashion as integration curtailment described next.

Curtailment (if relevant) at the point of integration is calculated for each grid cell using the wind profile of the cell, the net load curve and specific generation layers of the destination region (described in SI 3.1.1), to determine what fraction of the cell's

available wind can be utilized given demand conditions (described in SI 3.1.2). Curtailment results in a reduction in the amount of wind generated from that cell and a corresponding increase in the LCOE as the cost per kWh delivered increases (CurtCost). Reserve and ramping costs (ReRaCost) are calculated using the post-curtailment wind profile (described in SI 3.1.3 and 3.1.4).

Once all costs have been totaled for each of the six options, the cell with the lowest total cost of generation from wind is selected and added to the supply curve. The total available capacity in the chosen cell is installed after considering physical spacing and exclusion constraints, as described in in SI 1. In our illustrative example shown as Step (2) in Figure S1, one NW-NW grid cell offers the least-cost option for integrated wind. Bar widths on the supply curve correspond to differences in available land area and reductions in potential due to curtailment for a single cell.

Once a cell is added to the supply curve, the net load profile (in our example, the NW) and net transmission capacity profile are updated to reflect newly integrated wind shown as Step (3) in Figure S1. (In our example, the transmission profile is not updated because no inter-regional transmission is required.) The previously-used cell is marked as already integrated and unavailable for the remaining iterations of the model. The process of identifying the least-cost available source of wind from across the six options begins anew, repeating the above steps.

2.2 Generation Cost Model

The generation cost model determines the levelized-cost-of-electricity (LCOE) of wind prior to integration by using the capacity factor and financial assumptions for each grid cell available for siting wind.

LCOE represents the net discounted cost to install and operate a wind farm divided by its expected generation in its lifetime. In other words, the LCOE is equivalent to the break-even tariff that wind project developers would require to build and operate a wind farm in a given location. In addition to the availability of wind, it varies with capital costs, operational costs, and financial parameters. In practice, the LCOE can be compared to electricity tariffs to determine expected quantity, or can be used to establish a price (feed-in tariff) to support a desired quantity. This paper employs the former.

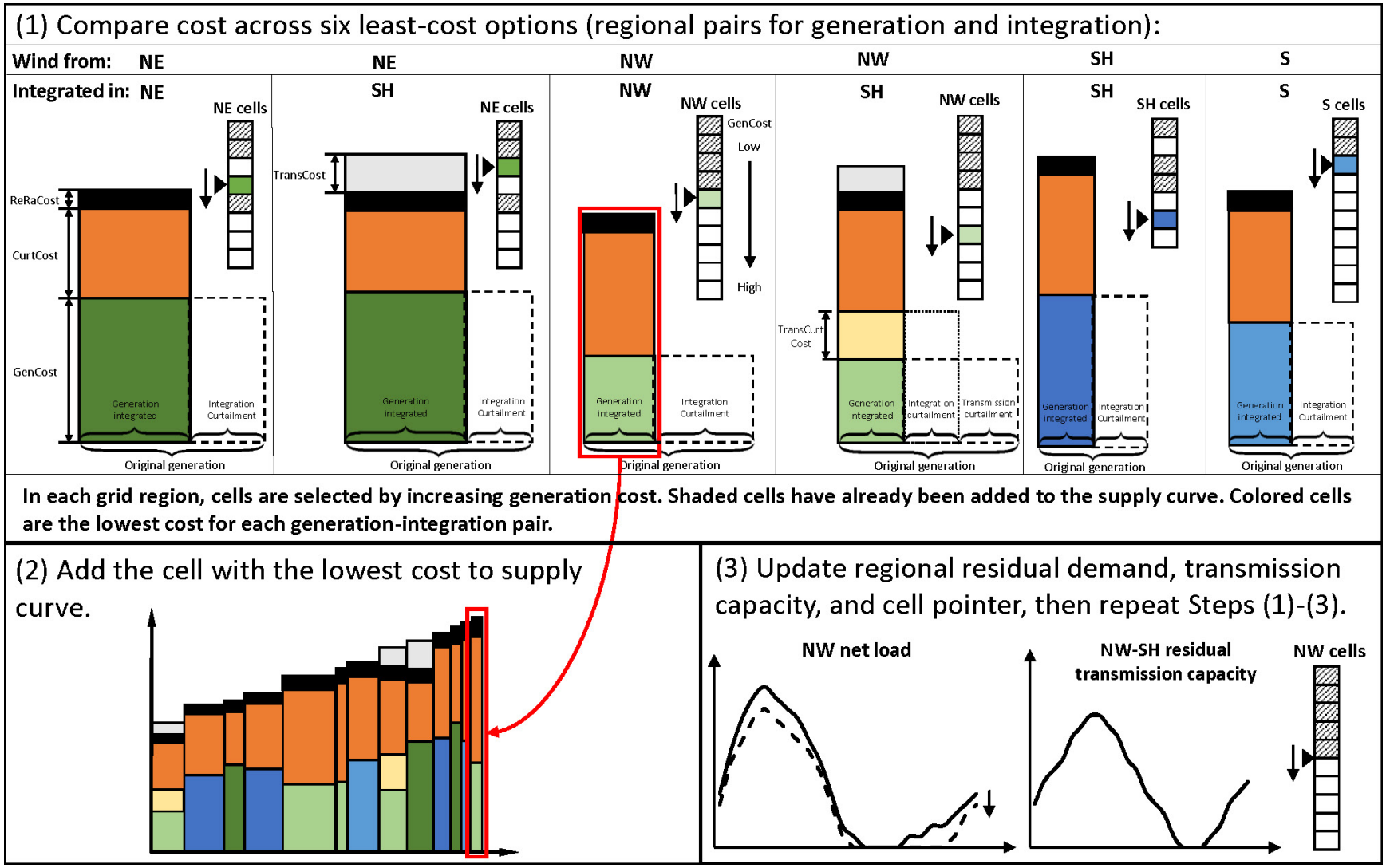

Figure S1. Overview of the routine used in wind supply curve construction.

The Chinese government offers wind projects a 50% reduction in the Value Added Tax (VAT) relative to projects in other industries, equivalent to 8.5% of total revenue. The VAT paid during the purchase of relevant equipment such as turbines and substations can be deducted from the VAT as well. Furthermore, the Enterprise Income Tax (EIT), which is set as 25% of the Income Before Tax (IBT), offers an additional incentive for wind farm investment. In the first three years after wind generation is initiated, the government guarantees full tax break from the EIT, and then provides for a 50% reduction in the EIT to 12.5% for years four to six[3].

The interest rate on the annual loan payment is assumed to be 6.2% (consistent with prevailing commercial rates in China) and the distributions for loan payments are assumed to remain constant over 15-year period in this study. The depreciation period is also set at 15 years. The detailed calculation methodology for NPV is described in following equations. The threshold price is determined when the total NPV, including prepaid investment and debt, capital cost, O&M cost as well as loan payment and tax is equal to zero. To simplify the variability of wind resource, the capacity factor for each grid cell is assumed to be constant during the lifetime of the wind turbine:

$$NPV = \sum_{i=1}^{N} Cash(i) \cdot (1 + IRR)^{-i}$$

where

NPV is the net present value,

$Cash(i)$ is the cash flow in year i,

IRR is the internal rate of return, which is set at 10%, and

N is the total lifetime of project, assumed here to be 25.

$$Cash(i) = Revenue(i) + Debt(i) - CapitalCost(i) - O\&MCost(i) - Loanpayment(i) - Tax(i)$$

$$Revenue(i) = Q(i) \cdot P$$

$Q(i)$ is the annual electricity production in year i (kWh), which equals to capacity multiplied by nameplate capacity and 8760 hours from the third year. In the construction period during the first and second year, $Q(i)$ is zero.

P is the sale price of wind electricity, with the assumption of a constant price over the project lifetime.

$$Debt(i) = \begin{cases} 0.8CapitalCost, & i = 2 \\ 0, & i \neq 2 \end{cases}$$

$CapitalCost$ is the overnight capital cost of wind project.

$$CapitalCost(i) = \begin{cases} 0.2CapitalCost, & i = 1 \\ 0.8CapitalCost, & i = 2 \\ 0, & i > 2 \end{cases}$$

We select 100 yuan/MWh as the average O&M cost over the lifetime of Chinese wind projects. Total annual O&M cost (yuan/kWh) is given by:

$$O\&MCost(i) = \frac{100 \cdot Q}{1000}, i \geq 3$$

$$Loanpayment(i) = \frac{Debt(2) \cdot r \cdot (1+r)^{15}}{(1+r)^{15} - 1}, \quad i = 3 - 17$$

where the interest rate $r = 6.2\%$ for the loan payment.

$$Tax(i) = VAT(i) + EIT(i) + Surtax(i)$$

$$VAT(i) = \frac{Revenue(i) \cdot 0.17 \cdot 0.5}{1.17}$$

$$Surtax(i) = 0.1 \cdot VAT(i)$$

where $VAT(i)$ is an 8.5% Value Added Tax in year i, and $Surtax(i)$ is the education and urban construction accessory component of Value Added Tax with a rate of 10%.

$$EIT(i) = \begin{cases} 0, & i = 1-5 \\ 0.125IBT(i), & i = 6-8 \\ 0.25IBT(i), & i \geq 9 \end{cases}$$

where $IBT(i)$ is the Income Before Tax in year i, calculated as following:

$$IBT(i) = Revenue(i) - InterestPayment(i) - O\&Mcost(i) - Depreciation(i)$$

$$InterestPayment(i) = Principal(i-1) \cdot r, \quad i = 3-17$$

$$Principal(i-1) = \begin{cases} Debt(2), & i = 3 \\ Principal(i-2) \cdot (1+r) - Loanpayment(i), & i = 4-17 \end{cases}$$

$$Depreciation(i) = \frac{CapitalCost}{15}, \quad i = 3-17$$

3. Economic Dispatch Model

3.1 Model Structure and Methodology

The dispatch model matches supply and demand on an hourly basis for the entire year. The annual electricity demand profile (preserving temporality) is partitioned in each hour to the generators according to a heuristic probable dispatch order. The heuristic gives preference to high fixed cost/low variable cost generation (typically, base load) as well as inflexible generators in terms of cycling. A must-run limit of generators in the base layer determines the level of curtailment due to integration. The costs of providing reserves to meet wind forecast errors are calculated according to which generators are supplying them. Generator responses to temporal fluctuations in demand are considered through the calculation of ramping costs for each generation type. We discuss each of these components in detail below, followed by a note on the advantages of our method over traditional "screening curve" approaches, and a discussion of potential errors introduced using this method.

3.1.1 Generation layers

Supply of electricity is arranged according to the probable dispatch order of generators. Similar to traditional planning models, generators with high fixed costs

relative to variable costs are dispatched first. These plants, in order to recoup their fixed investment and operating costs, need to run for longer periods of the year and are thus sometimes considered "base load" generation. By contrast, other plants with low fixed costs relative to variable costs in some cases may only come online during high demand conditions when the price to provide the marginal unit of electricity exceeds the cost of fuel and other limited fixed costs. These are referred to as "peakers". There exist other classifications on this spectrum. By assuming homogeneity within a given plant type, multiple plants can be combined into a single layer represented by the sum of capacities.

Distinct from traditional approaches, we also consider operational characteristics of generators to improve realism of the dispatch order for China. Some of these technologies—in China, nuclear and coal-fired power—have more restrictive operational requirements that limit how flexibly they can ramp up and down (known as cycling) or startup and shutdown. In addition, China has an unusually high-level of coal-fired combined heat and power (CHP) units that provide district heating to cities and cannot be shut down in the winter heating periods. The cogenerated nature of heat and electricity restricts the flexibility of the electricity produced by the units even further.

We thus introduce a new dispatch order of four layers (G1-G4) that allocates a portion of traditional base load plants to the base layer G1 and the remainder to a more flexible layer G3, which is the unused capacity of units in G1 as well as units of the same type not in G1. Hydropower, both a flexible and often base-loaded power source, is in G2. Natural gas units, considered as peaking, are in G4 (see Table S3). The size of these layers are adjusted throughout the year according to predicted availability described in the Data section below. For our purposes, we allow coal to encompass other potentially substitutable fuels such as biomass.

Table S3. Description of generator types for different generation layers

Layer	Generator types
G1	Nuclear, must-run coal
G2	Hydropower
G3	Remainder of coal
G4	Natural gas

The supply must meet an annual demand profile in each hour. This is achieved by partitioning the demand into generation layers according to dispatch order as illustrated in the figure. Generation is zero for any layer in hours when demand is less than the cumulative capacity below it, as shown in Figure S2.

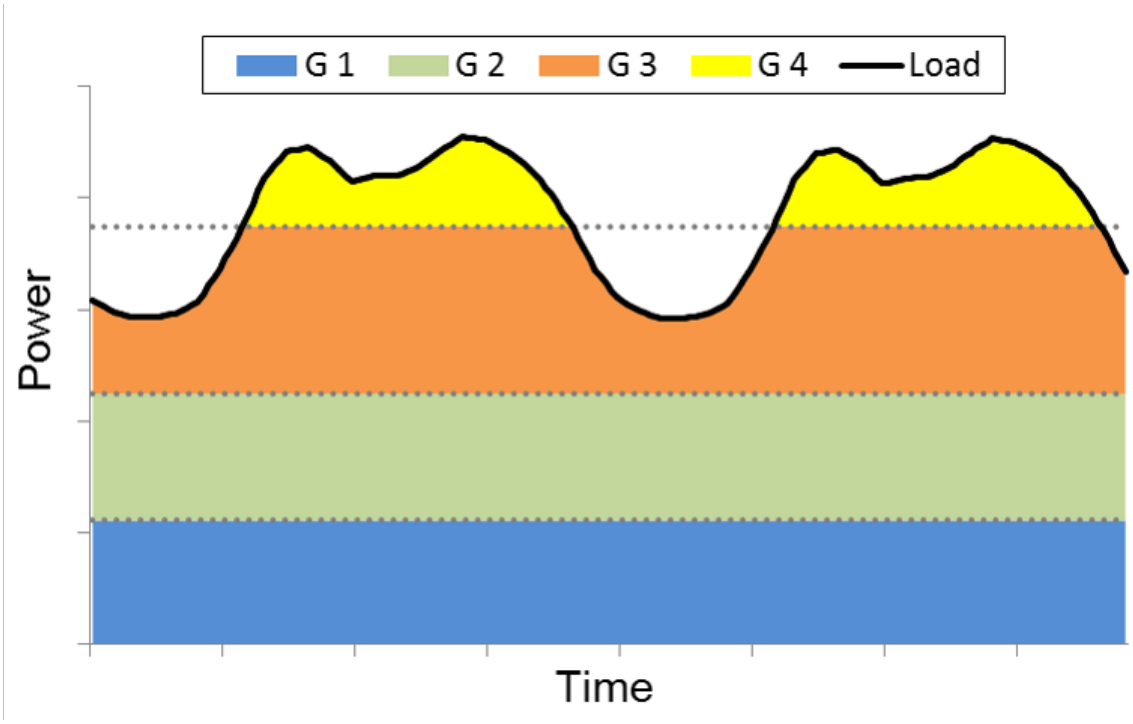

Figure S2. Dispatch model partitioning demand according to generation layers

3.1.2 Wind profiles and curtailment calculation

Wind power is intermittent and non-dispatchable, and hence cannot be represented by a generation layer. Instead, we construct a net load curve, the difference of demand (also referred to as load) and wind outputs, which is the remainder of the load that must be met by the conventional resources represented in the four layers. In addition, based on the construction of the layer G1, we curtail all wind that pushes net load below the must-run threshold (the patterned portion that dips into layer G1 in Figure S3).

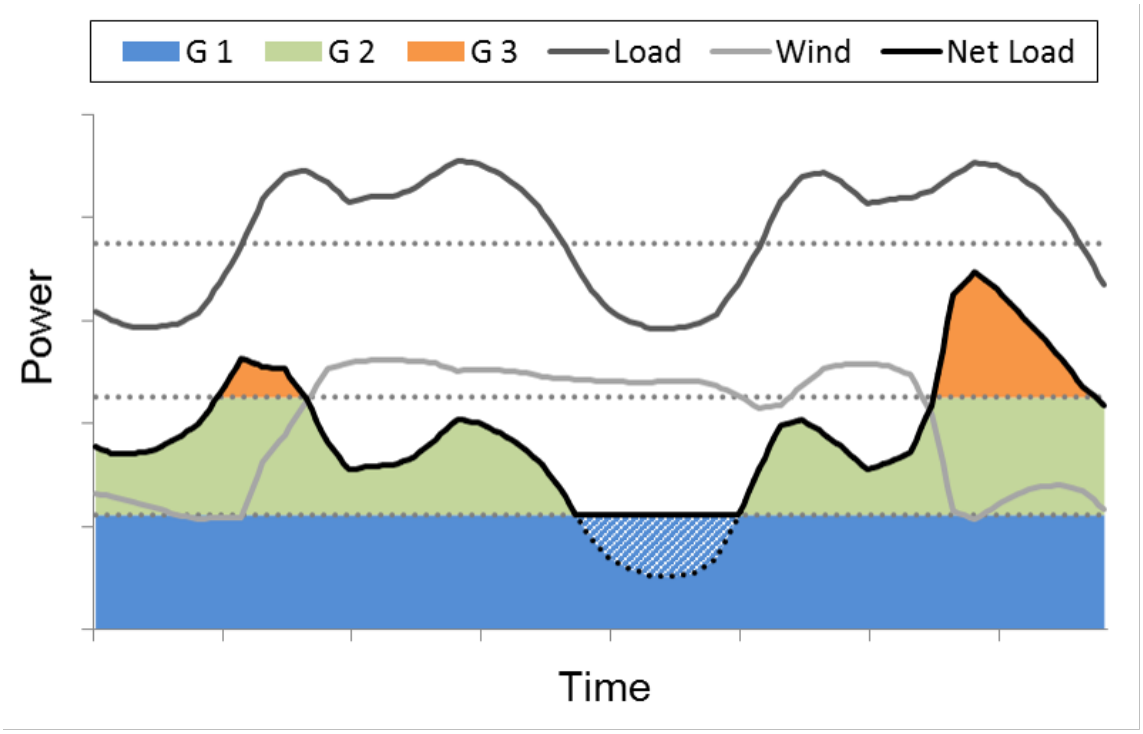

Figure S3. Dispatch model partitioning demand according to generation layers in the presence of wind (patterned areas indicate curtailed wind, when net load falls below the must-run threshold).

3.1.3 Reserve costs

Increasing penetrations of intermittent renewable energy require standby capacity (reserves) to be available for unexpected changes in output[4]. Calculation of this reserve requirement as a function of wind output is highly system dependent. A review of Chinese sources on various grid regions revealed ranges for reserve requirements (as a fraction of forecasted wind) that would not exceed 20%[5]. These references were used to bracket three scenarios for integration costs in this analysis.

Reserve requirements are met by generators in the same dispatch order above. Thus, an amount of "reserve generation" is added to the net load curve and allocated to the corresponding layer(s). Costs of reserve by generator type are described in the Data section below.

3.1.4 Ramping costs

Changes in output of conventional generators incur additional costs in terms of reduced efficiencies and increased wear and tear. As a single layer's capacity aggregates multiple units, large ramps may require startups or shutdowns of individual units as well. These costs are included in a further sensitivity described in SI 4.3.4. Our model estimates ramping costs by calculating hourly changes in output from each layer and multiplying by a range of ramping costs from the literature. To calculate those attributable to the presence of wind power, we use the difference between ramps of the load and net load (post curtailment).

3.1.5 Relationship to screening curve model

The "screening curve" approach is a traditional model used for expansion planning to determine optimal capacity mixes given the levels of demand and the respective fixed and variable costs of different generators. It relies on an abstraction of demand to a net load duration curve (NLDC), the ordering of demand by hour in a given year from highest to lowest. The concept is illustrated in Figure S4 below (note we have neglected the inclusion of non-served load for simplicity). From the number of hours for which a given type will be the most economic to meet demand (vertical lines in the figure), the appropriate amount of capacity of each type (G1-G4) is calculated.

The approach we adopt includes several advances beyond standard practice important to modeling grid-integrated economic wind potential. Fundamentally, the conventional "screening curve" model is used to calculate economic expansion of dispatchable generators, e.g. wind and other intermittent generation sources are not typically considered. This approach cannot endogenously select the appropriate amount of non-dispatchable wind capacity to build. Here we develop a more sophisticated setup that accounts for the non-uniformity of wind resources. Our method also considers seasonal differences in the availability and must-run capacities of different generation types, whereas the screening curve assumes constant availability throughout the year. Finally, our method explicitly accounts for inter-hourly changes through the calculation of ramping and associated costs, information that is lost when creating the NLDC.

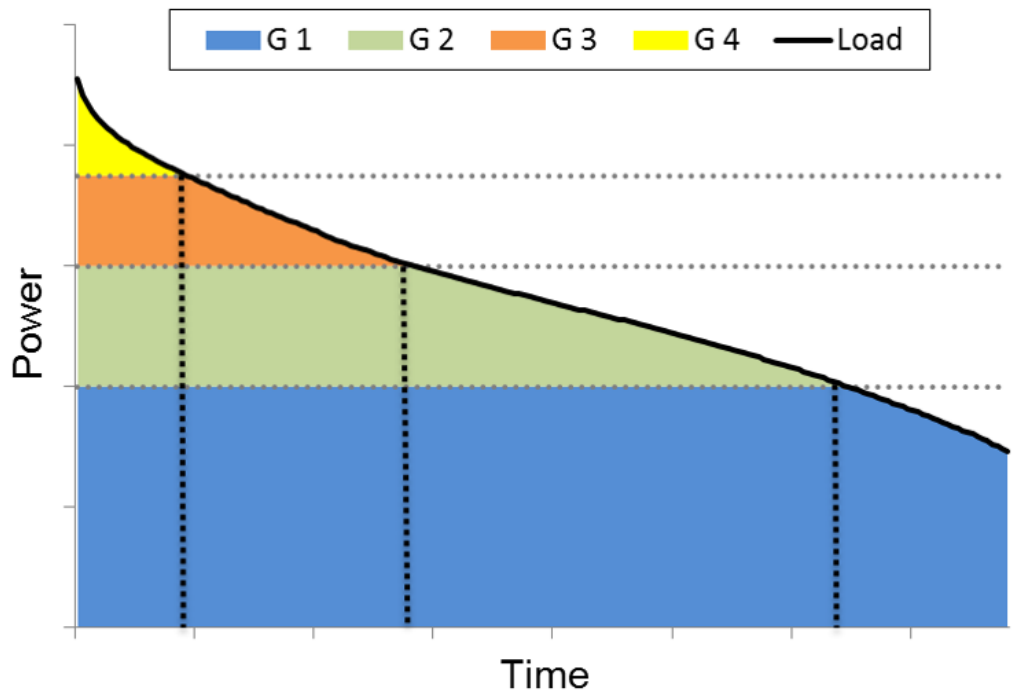

Figure S4. Traditional "screening curve" model using annual net load duration curve

3.1.6 Potential approximation errors

Determining the appropriate hourly generation amounts by power plant, assuming centralized operation, is in general a mixed integer linear program (MILP) optimization problem known as unit commitment and economic dispatch, accounting for a range of techno-economic criteria. For example, large fluctuations in wind may occur over the span of a few hours – less than an acceptable startup/shutdown time for a typical 600 MW coal-fired power plant or nuclear plant. These startup and shutdown decisions are discrete events. Minimum generation outputs of committed units further constrain the feasible region.

Outside of the base layer, our model approximates these instead as a continuum, (a) neglecting any potential infeasibilities in being able to meet low load or rapid changes in load, and (b) not explicitly counting the number of startups for the purpose of cost estimation. These would tend to overestimate the flexibility, or underestimate the integration costs of wind energy in higher generation layers.

At low net load conditions when wind is being curtailed, our reference case would conversely tend to underestimate flexibility by not allowing for the shutdown of units

regardless of projected wind availability. More flexible operation of coal plants, such as through "hot starts" that significantly decrease the required startup time by maintaining temperatures and pressures within the plant, would impact the integration potential. We examine this in our sensitivity on coal flexibility. An additional mechanism would be co-optimizing heat and electricity production to respond to daily fluctuations in heat demand.

The heterogeneity of plants that is ignored when creating the generation layers can influence dispatch by varying the startup times, ramp rates and other flexibility parameters. All else equal, our homogeneity assumption would underestimate system flexibility because a diversity of units would tend to create a larger feasible region of aggregate outputs.

3.2 Data

3.2.1 Generation layers

We use as our central case the projected capacities for nuclear, coal plus biomass (combined in this analysis; hereafter, referred to as coal+biomass), hydropower and natural gas in 2030 by State Grid, shown in Figure 5 and replicated in Table S4 below[6]. We assume average availability factors for these technologies of 100%, 90%, 40% and 90%, respectively. We further use projections of coal-fired combined heat and power (CHP) plants given moderate heating demand growth.

Table S4. Reference projections for 2030 capacities by region (GW)

Technologies	Nuclear	Coal+Biomass	Hydro	Gas
NE	14	152	18	5
NW	0	295	50	8
S	45	176	161	49
SH	92	737	302	138

These are allocated to the layers G1-G4 by each region as follows.

3.2.1.1 Layer G1 (Nuclear and must-run coal)

All of nuclear and the minimum operating points of Must-Run Coal (MRC) capacity make up layer G1. The MRC varies by region according to the penetration of must-run combined heat and power (CHP), minimum operating limits of committed

capacities, demand profiles, and availability of flexible generators to meet peak demand. Over each time period *t* (one week in our reference cases), we require that we have available sufficient reserve generators to meet peak load plus a reserve margin (set to 5% based on common practice and regulatory requirements in Northwest[7]):

$$Nuclear_t + MRC_t + Hydro_t + Gas_t \geq PeakLoad_t * (1 + ResMargin)$$

where Gas_t and $Hydro_t$ capacities are adjusted for availability. Coal units consist of:

$$MRC_t = MRC_{t,CHP} * Pmax_{t,CHP} + MRC_{t,Elec} * Pmax_{t,Elec}$$

where *Elec* refers to electricity-only plants, and *Pmax* are maximum power outputs.

Layer G1 of minimum loadings for must-run units is thus given by:

$$G1 = Nuclear_t + MRC_{t,CHP} * Pmin_{t,CHP} + MRC_{t,Elec} * Pmin_{t,Elec}$$

where *Pmin* are the (potentially time-varying) minimum outputs, and *Nuclear* is assumed to run at full capacity.

CHP plants have reduced flexibility in terms of electricity outputs under high heating loads (and in the case of smaller back-pressure units, electricity output may essentially be fixed). In terms of minimum and maximum electric power, we have the relation:

$$Pmin_{Elec} \leq Pmin_{CHP} < Pmax_{CHP} \leq Pmax_{Elec}$$

The must-run CHP fleet parameters are benchmarked against multiple data sources for the Northeast, e.g., in 2011: CHP must-run capacity was 18.2 GW, total CHP capacity 27.6 GW and total coal capacity 58.9 GW, translating to 65.9% average minimum power outputs[8]. Additionally, heating seasons are generally divided into three parts, with the middle (roughly December-February) representing the peak of heating demand, and the early and end having minimum electricity outputs roughly 15% lower. We therefore let:

$$Pmin_{t,CHP} = \begin{cases} 65\% & Dec, Jan, Feb \\ 55\% & Oct, Nov, Mar \end{cases}$$

Similarly, high heating loads mean that maximum electricity outputs are reduced:

$$Pmax_{t,CHP} = \begin{cases} 90\% & Dec, Jan, Feb \\ 100\% & Oct, Nov, Mar \end{cases}$$

We assume modest growth of CHP through 2030, with 300GW installed and roughly comparable distribution geographically to the present (allowing for some relative increases in the NW), with modeled capacities in Table S5.

Table S5. CHP capacities (GW) in 2012 and 2030 (projected)

	2012	**2030**
SH	157	214
NE	48	56
NW	15.5	30
Total	220	300
Source:	CEC (2013)	THUBERC (2015)

Minimum generation points of electricity-only coal-fired generators are the subject of much debate in China. From a technical standpoint, even the most advanced units can ramp down to 40% or lower of their rated capacity. As this may affect the efficiency of the plant, where markets exist coal plants may choose different economical generation limits. In practice in China, minimum outputs used by the grid operator are fixed administratively and may not represent either technical or economic minima. These typically do not go below 50%. Appropriate minima are topics of research discussed in the latest electricity reform plans, because of the high inflexibility in integrating renewable energy[9]. We let $Pmin_{t,Elec} = 50\%$ and $Pmax_{t,Elec} = 100\%$ in our reference case and perform sensitivities around this flexibility parameter.

Finally, we use expected export-designated capacities to shift where capacities are counted, reflecting the likelihood of joint dispatch of these plants with those in the receiving region. Extrapolating from 2020 power export projections[6], we set export capacities in 2030 to be 28 GW and 90 GW for the NE and NW, respectively, and a net import capacity of 118 GW in SH. This increases the availability of electricity-only coal-

fired power, but does not directly affect the calculation of the must-run layer. There is very limited predicted inter-regional transmission into or out of the S.

3.2.1.2 Layer G2 (Hydropower)

Because of seasonal variation in the availability of water, we scale hydro generation layer capacities using historical averages (2008-2014) of monthly hydropower generation, reaching average capacity factors for hydropower of roughly 40%[10]. In doing so, we allow for more hydropower generation during periods of high rainfall, primarily in the spring and summer months, see Table S6.

Table S6. Hydropower capacity factors by region and month, constructed from average monthly consumption in 2008-2014.

	Jan	Feb	Mar	Apr	May	Jun	Jul	Aug	Sep	Oct	Nov	Dec
NE	0.27	0.28	0.34	0.37	0.49	0.59	0.53	0.53	0.44	0.36	0.30	0.30
NW	0.24	0.21	0.26	0.36	0.45	0.50	0.53	0.57	0.52	0.45	0.39	0.32
S	0.25	0.21	0.27	0.29	0.37	0.46	0.59	0.62	0.53	0.47	0.39	0.36
SH	0.25	0.23	0.28	0.33	0.42	0.50	0.57	0.57	0.53	0.43	0.37	0.31

3.2.1.3 Layers G3 and G4 (Remaining coal and natural gas)

The remainder of available coal capacity after removing must-run capacity for G1 is placed in G3. This is the primary region of ramping and reserves. Natural gas forms the final layer G4. An example output of this algorithm is shown for the SH reference case in Figure S5.

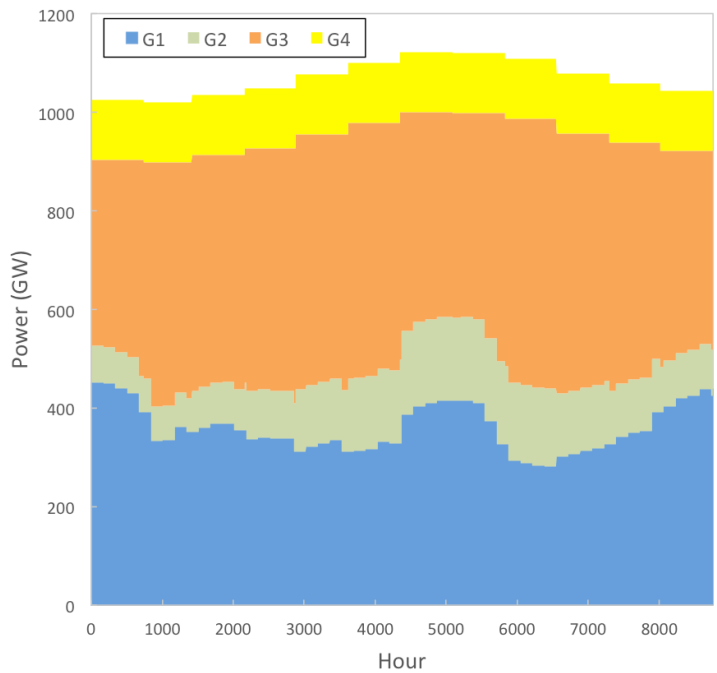

Figure S5. Generation layers for Sanhua reference case

3.2.2 Demand Profiles

Given that we do not have access to complete records of hourly or intra-hourly demand behavior in China, we develop a procedure for reconstructing demand profiles from available data that capture important sources of variation in load, including: 1) seasonality of electricity and heat demand (Chinese New Year, as well as the calendar seasonality of heating requirements in residential and industrial facilities) and 2) daily variability driven by different load profiles in regions (e.g., industrial, commercial and residential demands).

We then construct a full 8760-hour load curve for each of the four grid-regions of China as follows:

(1) Calculation of daily normalized load profiles

For each of the three State Grid regions (NE, NW, SH), we sum the typical seasonal load curves of provinces in the region for year 2010 (both winter and summer). These are then normalized (i.e., sum to unity over the day) into typical daily profiles: six in total. The original source of the data is China's State Grid Corporation, and was obtained

through a consultancy[11]. The data are provided on hourly basis for a typical summer and a typical winter day.

For the South, we obtained an hourly profile of Guangdong's electricity consumption in 2010 from Southern Grid[12]. We create a typical daily curve for winter and summer by averaging at each hour of the day. We use April-Sept for summer and the other months for winter. We normalize these two to obtain typical daily load profiles as above.

(2) Construction of full year demand profiles

We use daily total consumption data by province available from the State Electricity Regulatory Commission for the period August 2012 – June 2013 to scale up our normalized daily profiles and generate a full year series[13].

We fill in gaps by assuming continuity in load profiles and interpolating values for unavailable data points. Based on monthly consumption totals, we approximate July data from June and August because daily data were not available for July, ensuring that total annual generation is consistent with aggregate statistics.

Consumption in 2013 grew roughly 8% over 2012, and we use monthly year-on-year consumption growth by province to adjust our August 2012-August 2013 to a 2013 calendar year series[13].

(3) Scaling to 2030 demand conditions

As done in the original version of this manuscript, we take the yearly profiles by region generated for 2013 and scale to 2030 according to projected regional electricity demand growth forecasts by the State Grid Corporation[6]. This results in the following increases: NE: 91.2%, NW: 134.8%, SH: 74.0%, S: 74.0%.

Demand projections used for this analysis assume a 2-3% annual load growth in 2030. Given the 8% annual load growth observed in 2013 over 2012 that would tend to upwardly bias end-of-year consumption, we apply a correction factor. Specifically, we shift consumption later in the year downward and consumption earlier in the year upward to obtain an annual profile with roughly 3% growth (as measured by near beginning and end of year data), while preserving seasonal differences in load.

3.2.3 Generator costs of flexibility (reserves, ramping)

A review of Chinese sources on various grid regions revealed ranges for reserve requirements (as a fraction of forecasted wind) that would not exceed 20%[5]. Reserves are currently largely uncompensated in China. However, recent reforms indicate that there may be pilots in flexibility products, which could feasibly include the capability of responding to changes in system conditions[9]. Due to chronic overcapacity in the sector, however, these reserves would likely lead to relatively low prices if markets were created.

Wind and other intermittent generation are expected to increase costs of net load following for conventional generators, as a result of increased heat rates and maintenance costs. Based on surveys of super-critical coal plants in the U.S., typical ramp rates of ~33% of capacity per hour result in additional costs of $1.5-$2.5 per MW capacity. This is equivalent to $4.5-7.5 per MW per hour (MW/h) ramping. Faster ramp rates may increase this by multiples of 1.5 up to 10[14]. We would expect maintenance costs in China to differ from the U.S., similar to overall differences in costs of construction.

These were used to bracket three scenarios for integration costs in this analysis (see Table S7).

Table S7. Integration cost parameters.

Costs by technology	Sensitivities (yuan/MWh)		
	Low	Base	High
Ramping costs			
Coal/biomass	50	20	10
Nuclear	-	-	-
Hydro	0	0	0
Gas	10	4	2
Reserve costs			
Coal/biomass	50	25	10
Nuclear	-	-	-
Hydro	0	0	0
Gas	50	25	10
Reserve requirement	20%	15%	10%

3.2.4 UHV transmission costs

We assumed transmission of wind energy between grid regions relies on ultra-high voltage direct current (UHV-DC). Further, we considered only the two expected

large volume wind transmission corridors: from the northwest (NW) and the northeast (NE) to "*Sanhua*" (SH) – Central China Grid (CCG; Henan, Hubei, Hunan, Jiangxi, Chongqing, Sichuan), East China Grid (ECG; Shanghai, Jiangsu, Zhejiang, Anhui, Fujian) and North China Grid (NCG; Beijing, Tianjin, Hebei, Shanxi, Shandong, West Inner Mongolia). The 800-kV transmission line from East Inner Mongolia to East China Grid with 10 GW capacity and 1800 km distance was selected as the representative project for wind transmission from NE to SH, with 3000 RMB/kW capital costs[15]. The 800-kV DC transmission project from Jiuquan to Central China Grid with 8 GW capacity is assumed to represent the wind energy transportation from NW to SH, with 3500 RMB/kW capital costs[16]. Annual O&M cost for both projects are assumed to be 1.5% of capital cost. These relatively high capital costs reflect the possibility that UHV cost could be much higher than expected due to insufficient capacity utilization and lack of a power market to encourage cross-region trade[17,18].

The transmission cost for wind energy is calculated based on the annual payback for transmission lines investment and the annual operation cost. We assumed a 10% internal return rate and 6.2% interest rate within 25-year financial time horizon. The equity share in capital cost is expected to be 20% and the calculation method is same as that in the cost model for wind projects in SI 2.2. The transmission costs on an energy basis will be sensitive to the realized loading, given that fixed dominate variable costs. Increasing transmission capacity to accommodate additional wind at high penetrations would reduce loading; thus, with a minimum fixed loading as a constraint, the maximum transmission line capacity is determined by the generation from wind and (fixed) planned thermal generation for export. Starting with capacity export projections from State Grid Energy Research Institute for 2020 and extrapolating to 2030 based on expected growth and export-designated plant capacities, available transmission line capacities for inter-regional wind were set as in Table S8.

Here we assumed that utilization full load hours of UHV-DC transmission is 4000 hours (46%) in the base scenario, resulting in UHV costs for NE-SH and NW-SH of 0.095 and 0.111 RMB/kWh, respectively. Acknowledging that realized loading—and hence, average cost per unit electricity transmitted—is uncertain, we elaborate our sensitivity ranges in SI 4.3.6.

Table S8. Projected 2030 transmission line capacities (GW) by export source and fuel type[6].

Transmission Pathway			Projections		Modeled
			Coal	Wind	
NE	→	SH	28	56	56
NW	→	SH	90	61	100

4. Sensitivities

We evaluate sensitivity of wind potential to changes in model structure and parameters that represent additional sources of system complexity. We discuss sensitivities for physical potential (total generation assuming maximum deployment), economic potential (total generation under cost constraints exclusive of integration constraints and costs), and grid-integrated potential (total economic generation inclusive of integration constraints and costs). Throughout, the convention *base [low, high]* is used to denote the base case and two extremes, where *low* and *high* refer to the extremes that minimize or maximize, respectively, the total available wind potential for an empirically-grounded set of parameter assumptions.

Sensitivities included in the paper are discussed in 4.1 and 4.2. We also conduct several additional sensitivity exercises to explore the robustness of the results in 4.3. These include sensitivity to various coal flexibility parameters, benefits of energy storage, demand response, cycling cost, low CHP growth, different UHV cost assumptions, and solar expansion.

4.1 Physical sensitivities

Based on available Chinese project data *(see Supplementary Materials 1.2*) and experimentally observed power fall-offs of turbine spacings of up to 7-10 rotor diameters[2], this paper uses a turbine spacing density for onshore wind installations of *2.58 MW/km^2 [1.5, 4.5].* The base case is equivalent to 0.58 km^2 area per turbine, or roughly 9×9 rotor diameter spacing. Offshore turbine spacing density is *5 MW/km^2 [4.5, 5.6]*, and based on projects to date as well as future "deep sea" threshold[1], we consider allowable water depths of *50 m [20, 100]*.

4.2 Economic sensitivities

The LCOE threshold represents the central planner's willingness to pay, inclusive of integration costs, to generate electricity from wind. We take *0.60 yuan/kWh* as our reference value and report wind potentials under alternative assumptions of *0.50* and *0.70* yuan/kWh, based on the current range of the wind FIT and potentially higher integration costs necessary to meet government targets. We do not consider preferential tariffs for offshore compared to onshore wind, capturing recent comparable offshore wind project concession prices and our goal of evaluating least-cost options. The full wind potential at a range of cost thresholds can be identified in Figure 3.

Capital costs are taken to be *7000 yuan/kW [8000, 6000]* for onshore and *13,000 yuan/kW [16000, 10000]* for offshore[19]. Since most wind installations in China are still under warranty, the available record for operation and maintenance (O&M) costs is limited. We select *100 yuan/MWh [150, 50]* for both onshore and offshore O&M costs, expecting a significant drop for offshore in the coming years[19].

Based on the UHV cost calculation in SI Section 3.2.4, the sensitivities tested are *0.11 yuan/kWh [0.147, 0.088]* and *0.095 yuan/kWh [0.126, 0.076]* for NW-SH and NE-SH, respectively.

4.3 Grid-integration sensitivities

4.3.1. Coal flexibility sensitivities

Economic wind potential is most sensitive to assumptions on the system operation and flexibility of coal generators, among the parameters tested in this analysis. In creating the must-run base layer, we isolate three important parameters: minimum loading of traditional coal-fired power plants, ability/willingness of combined heat and power (CHP) units to operate flexibly responding to system conditions, and coal unit commitment scheduling flexibility.

We take as a reference case that China's system dispatch in 2030 will be organized to meet demand at lowest cost respecting various techno-economic criteria. When prices reflect underlying marginal and opportunity costs, generators will be incentivized to operate flexibly. Given the relatively weak links in China's current system

between costs and price, we expect that as more market-oriented mechanisms are introduced these technical limits will become more relaxed and dynamic, as has occurred in many other systems following restructuring.

For our main sensitivity analysis we construct three scenarios – *CoalFlex, Reference* and *CoalRigid* – encapsulating combined assumptions on expected extreme ranges of these parameters. We develop these below and report more extensive results of the effects of modifying individual parameters on wind potential.

4.3.1.1 Minimum loading of electricity-only coal plants ($Pmin_{Elec}$)

Coal plants have minimum generation points below which combustion may become unstable and additional costly auxiliary fuel is required. Efficiencies will also decline as output decreases[20], leading to an economic threshold above the purely technical limit. These thresholds may go as low as 40%, though current practice in China places the average number used by system operators between 50% and 60%[21]. We use 50% as our reference, and a range of 40% to 60%.

4.3.1.2 Flexibility of CHP unit operations

CHP plants have reduced ranges of technical electric power limits, though flexibility does exist, and is already implemented by considering jointly electricity and heat demand in regions such as Denmark. In our reference case, adjusting for heat demand by time in the heating season, we allow for flexible ramping elaborated in SI 3.1.4.

In China, many CHP unit operations are scheduled in a relatively inflexible manner by setting an electric power output based on projected heat demand and not allowing this unit to participate in load balancing. We simulate this in our *CoalRigid* scenario, letting $Pmin_{CHP} = Pmax_{CHP}$.

4.3.1.3. Coal unit commitment scheduling flexibility

Similar to minimum generation points, starting up and shutting down coal units involve a set of techno-economic criteria. For example, “cold”, “warm” and “hot” starts (corresponding to temperatures maintained while offline) may require anywhere from 2-8 hours from a strictly technical perspective, though frequent cycling induces additional

maintenance costs. Hence, coal units do not typically cycle on and off on a daily basis. Traditionally, coal units operated at relatively constant output, but due to changing system conditions, an increasing number of plants engage in "two-shift operations", involving shutting down on a regular basis, e.g., over the weekend.

Scheduling generator startups in a least-cost manner is a key system operation function. It is common practice in China's major grid regions to fix commitment schedules a month or more in advance, and ensure that unit uptime is at least one week and typically much longer[21].

These two aspects of scheduling flexibility at the unit and system level are incorporated in the calculation of the must-run base layer according to the time horizon over which peak load is calculated. In our reference case, we ensure that peak load over the week is met, from must-run units with costly startups as well as flexible generators, hydro and gas, which we model without minimum output or startup constraints. In our *CoalFlex* case, we consider a situation in which available reserves must meet peak load over each 8-hour period, allowing for changes (commitments) between successive periods. We also report results for the case of meeting daily peaks.

4.3.1.4. Results

Table S9 summarizes our three main sensitivity cases, selecting the set of case assumptions that lead to the lowest and highest wind integration based on a full factorial analysis shown in Table S10.

Table S9. Sensitivity cases reported in main text, with detailed assumptions about minimum coal unit output, CHP output, and scheduling horizon. (PWh)

Main Coal Flexibility Scenarios			
	CoalFlex	*Reference*	*CoalRigid*
$Pmin_{Elec}$	40%	50%	60%
CHP output	Flexible	Flexible	Fixed
Scheduling	8-hr peak load	Week peak load	Week peak load
Wind Potential	**3.05**	**2.59**	**2.07**

Table S10. Coal flexibility cases with full factorial variation of $Pmin_{Elec}$, CHP flexibility, and scheduling horizon assumptions. (PWh)

Full Coal Flexibility Cases			
	$Pmin_{Elec}$		
	40%	50%	60%
Flexible CHP output			
8-hour peak scheduling	3.05	2.83	2.60
Day-peak scheduling	2.94	2.65	2.35
Week-peak scheduling	2.89	2.59	2.26
Fixed CHP output			
8-hour peak scheduling	2.94	2.68	2.42
Day-peak scheduling	2.80	2.49	2.14
Week-peak scheduling	2.76	2.42	2.07

Highlighted cells: *CoalFlex, Reference, CoalRigid*

4.3.2 Sensitivity to Pumped Hydropower

We estimate the potential impact of pumped hydropower and other energy storage options by taking the wind profiles in the base case supply curve and simulating discharging and charging to avoid curtailment, respecting power limits (the nameplate capacity) and energy volume limits (capacity available over 8 hours)[22]. Efficiency losses of 30% (typical for pumped hydropower) are assumed. Capacities are projected to be 10, 10, 21 and 60 GW for NE, NW, S and SH, respectively[6].

The simulation proceeds as follows for each region separately: in each hour, the net load is either above the minimum base load, or else it is at the minimum and wind is potentially being curtailed. If it is above, the pumped hydro storage will discharge to meet available demand at a power not greater than its rated power, until it is fully empty or there is no longer surplus demand. If the load minus the pre-curtailment wind profile is less than base load, then the storage will charge (up to its power capacity), until it is fully charged or the curtailment situation ends. The simulation proceeds sequentially through the year, charging and discharging, summing the total avoided wind curtailed. A sample of the effect on net loads in SH is shown below in Figure S6. Where net load with storage (blue) is below net load (red), additional wind power is allowed onto the system to be

charged. When net load with storage is above net load, storage is being discharged (to the extent possible without causing additional curtailment). The resulting wind potential increases to 2.66 PWh, a 2.4% increase over the base case.

This simulation makes a number of simplifications that would tend to overestimate the flexibility of the storage. In particular, it does not account for other functions of the pumped hydro such as providing peaking services, and it does not impose any additional restrictions such as to provide a minimum of reserves for reliability reasons. It also ignores uncertainty of hydro inflows.

The output of this simulation is a particular storage profile of charging and discharging that reduces wind curtailment. However, because the wind supply model cannot endogenously select the storage profile, there may be a better grouping of wind cells to take advantage of these storage options.

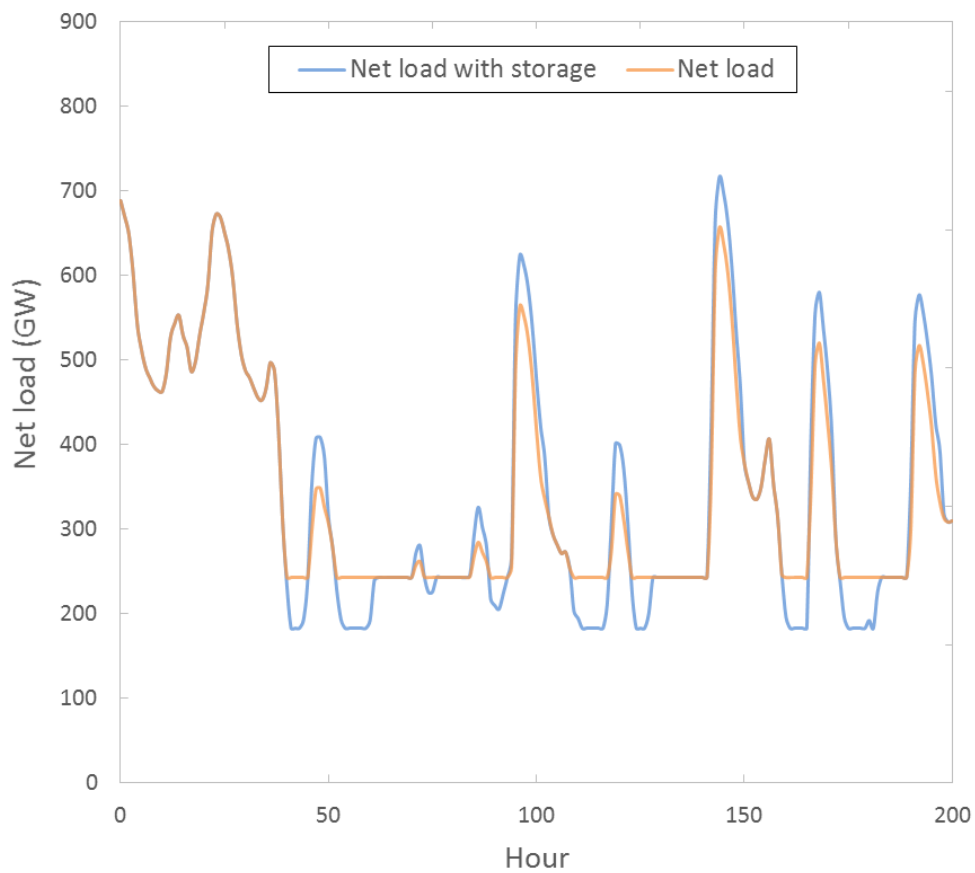

Figure S6. Net loads with and without energy storage for sample week in SH

We employ an iterative algorithm to improve our wind cell selection in the presence of storage. Following the storage simulation, we create a demand curve with the storage profile fixed (considering charging an increase in demand, and discharging a decrease) and rerun the wind selection model. This generates a new set of wind cells adapted to the particular storage profile. We iterate this procedure 20 times, and find that improvements as a result of storage reach 2.81 PWh, or 8% above the base case without storage (see Figure S7).

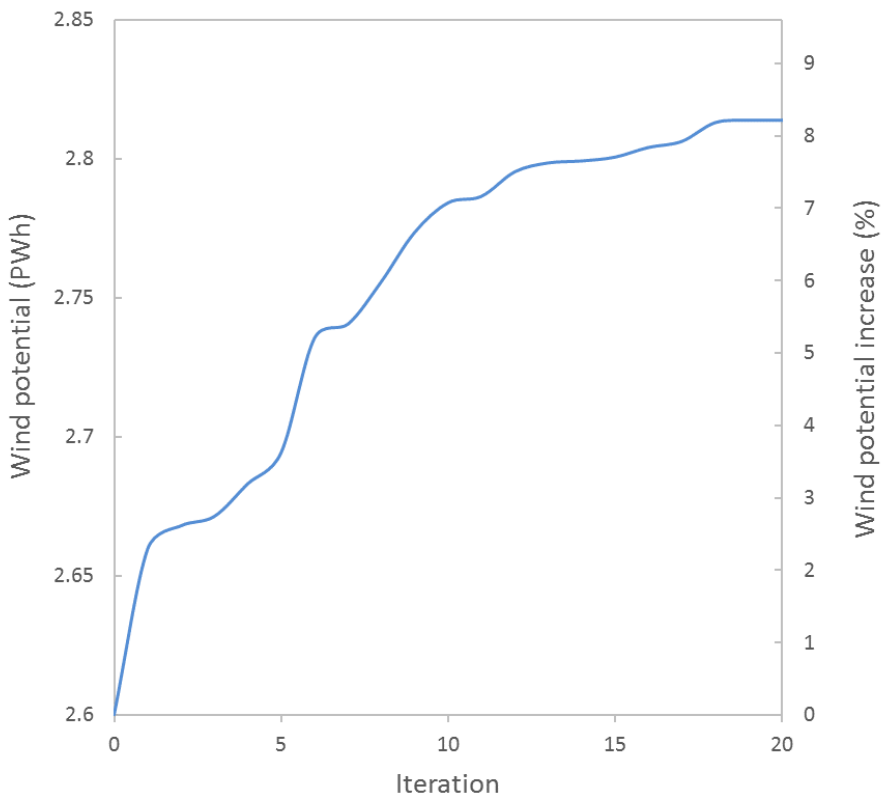

Figure S7. Wind potential increases as a result of endogenizing storage profiles

Importantly, this analysis ignores the economics of using energy storage to integrate wind power, which may not be as viable as the simple arbitrage mechanism modeled here. To achieve this 8% improvement would require significant improvements in operation and compensatory schemes for flexibility. For example, current pumped hydropower installations in northern China to integrate wind power are uneconomical in the absence of pricing reforms[23].

4.3.3 Sensitivity to Demand Response

The overall purpose of demand response in China (and most other locations) is to provide extra flexibility during system peak conditions, not explicitly to integrate renewable energy. A version of this demand response, critical peak pricing, is already implemented in many regions of China[24]. Early experiments in Shanghai suggest that potential peak reductions of 4% are possible from commercial and industrial customers[25]. Creating incentives to respond to intermittent wind supply conditions (and hence, endogenizing demand response into our wind selection method) would require significant additional infrastructure, including most likely real-time pricing.

We simulate this additional sensitivity by constructing different load profiles. We imagine a spectrum with two extremes parameterized by α ($0 \leq \alpha \leq 1$): when $\alpha = 0$, we have our base case load profiles; when $\alpha = 1$, we have a flat load profile such that power is constant over each day and equal to the average for that day's total consumption. (We do not consider multi-day load shifting.) We also test the intermediate value $\alpha = 0.5$ as a weighted sum of these two as illustrated in Figure S8 for a summer day in SH.

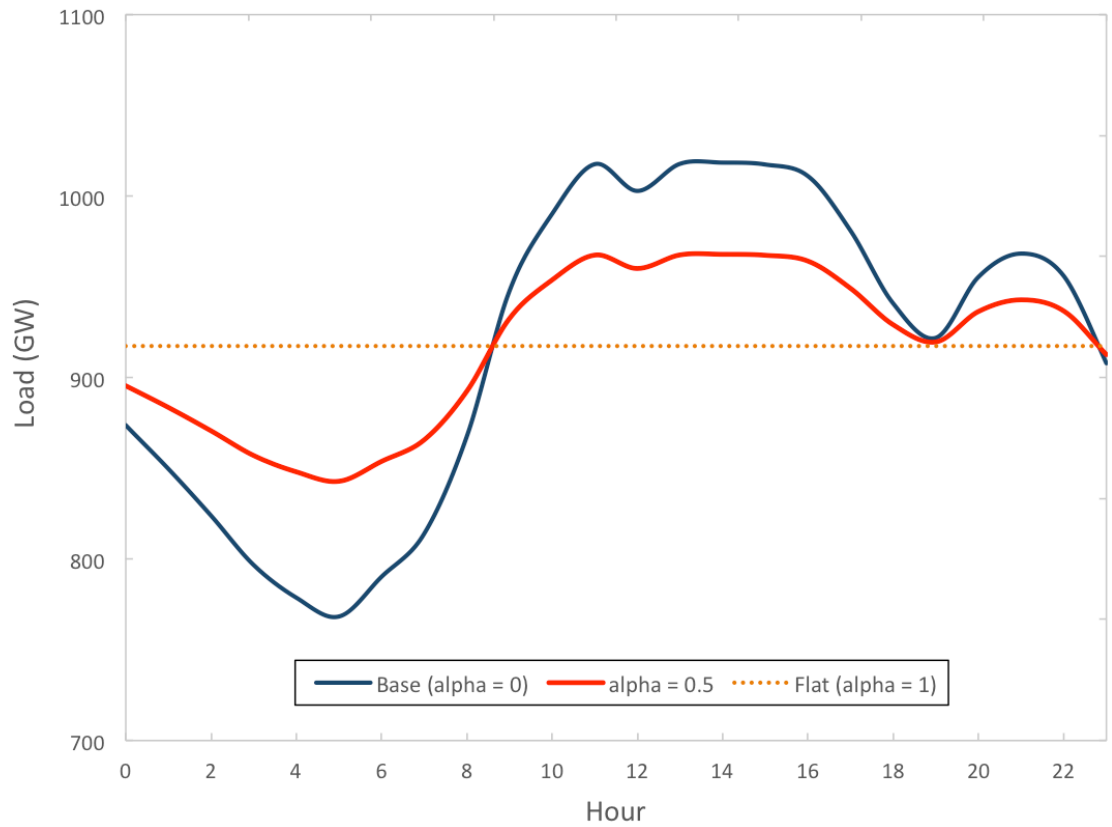

Figure S8. Example of range of demand response profiles tested, for summer day in SH.

We find that wind potential under $\alpha = 0.5$ (corresponding to a 5% peak load reduction on the peak summer day of SH) increases 6.6%, to 2.77 PWh. Under the extreme case of a flat daily profile ($\alpha = 1$, corresponding to a 10% peak load reduction), wind potential increases 10.8%, to 2.89 PWh. More flexible coal unit scheduling to meet eight-hourly peak loads rather than weekly (see SI 4.3.1 for description of this sensitivity) already captures much of these benefits: improvements under this more flexible commitment scheduling regime of shifting the reference daily profile to $\alpha = 0.5$ are only 2.7%. These demonstrate that under realistic assumptions on peak load shifting, wind potential can be improved to some extent.

4.3.4 Sensitivity to cycling costs

We examine the sensitivity of our results to startup costs by adjusting ramping cost parameters. The costs of starting up a unit depend on the boiler technology, fuel and

length of time offline. They are also difficult to estimate because a portion of these costs come from long-term maintenance and reliability impacts. Median startup costs for a hot, warm and cold start of an ultra-supercritical boilers have been reported at $54, $64 and $104 / MW, respectively[14].

Our range for ramping costs of coal-fired units tested was 20 *[10, 50]* yuan per MW/h. As an implausibly extreme case, a drop in power would require the shutdown of a unit of the same capacity, and a rise a startup. Adding per MW warm start costs to our base estimate of coal power output ramping costs, we arrive at 423 yuan per MW/h, or a 20-fold increase over the base case. Interestingly, this results in 2.54 PWh, or only a 1.9% reduction from the base case. We reconstructed the supply curve under these new assumptions (shown in Figure S9), which shows that the effect of altering the ramping cost assumption is mostly inframarginal, i.e., it does not have a strong influence on the marginal wind cells at modeled LCOE thresholds, inclusive of all costs. Curtailment-related integration costs increase rapidly above LCOEs of 0.4 yuan / kWh, which dwarf reserve, ramping and other costs. Changes in the optimal location of wind farms resulting from the adjustment to the ramping costs across regions are minor. In other words, the overall impact of this 20-fold cost increase in ramping costs is very modest.

A more complicated ramping formulation (e.g., considering startup costs) is expected to increase the cost of marginal wind cells at substantially reduced LCOE thresholds. For example, at 0.4 yuan/kWh (below our lowest LCOE threshold sensitivity), we find a reduction of 18% below the base case, from 1.27 to 1.04 PWh. At higher penetrations, actively curtailed wind can provide inexpensive upward ramping capabilities because of underutilized capacity if grid restrictions are lifted.

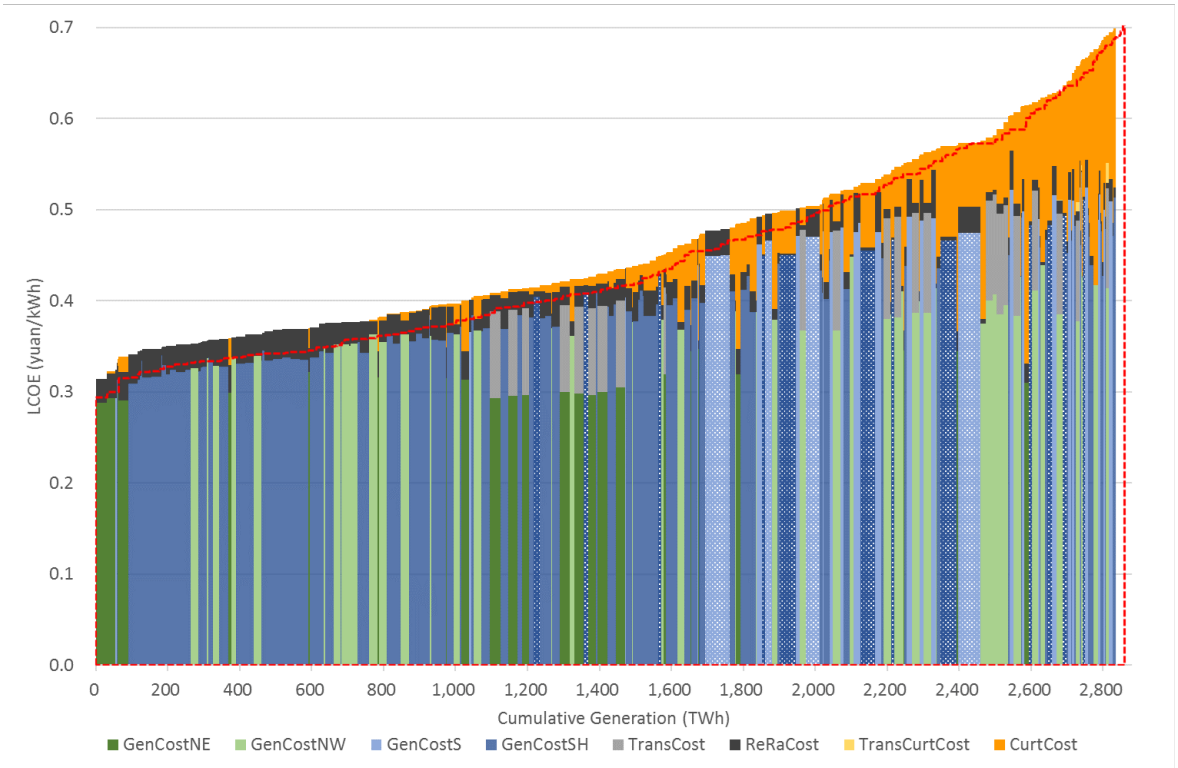

Figure S9. Wind supply curve in the high cycling costs scenario. Red dashed curve is the supply curve in the base case.

4.3.5 Sensitivity to CHP growth

The capacity of CHP is determined by heating demand, district heating policies and availability of alternate technologies. Our reference projections of CHP capacity growth to 2030 results in 300 GW installed nationally, which assumes some low-efficiency coal boilers are replaced by new installed or retrofit CHP units[26]. This is a relatively modest increase (2% annual growth) compared to 220 GW in 2012[27].

We construct a Low CHP case of 250 GW installed, under alternative assumptions of more deployment of alternative heating technologies such as industry surplus heat recovery as well as the improvement of heat utilization efficiency like mandatory energy codes for building construction[28]. Capacities by region in the Reference and Low CHP cases are shown in Table S11.

Under reference assumptions of coal flexibility, Low CHP only results in a wind potential increase of 0.3%, indicating that electricity demand growth (common to both cases) is expected to have a larger impact on must-run levels than much slower CHP

growth. The difference increases up to 1% as coal becomes more inflexible under the assumptions considered in SI 4.3.1.

Table S11. CHP Capacities in 2030 for Base Case and Low CHP Case (GW)

	Base	Low CHP
SH	214	178
NE	56	47
NW	30	25
Total	300	250

4.3.6 Sensitivity to UHV transmission cost

In calculating the cost of inter-regional UHV transmission (NE-SH and NW-SH), we have taken 46% utilization as our reference case. This parameter depends on various conditions of availability of supply at the sending end and coordination with receiving end. With higher penetrations of non-dispatchable wind, the utilization may decrease. For our main UHV sensitivity, we take as optimistic and pessimistic utilization scenarios 5000 hours (57%) and 3000 hours (34%). Based on this, low UHV cost scenarios for NE-SH and NW-SH are 0.076 and 0.088 yuan/kWh. High UHV costs are 0.126 and 0.147 RMB/kWh, respectively. We note that according to current grid plans, some of the SH intra-regional transmission interconnections assumed in the model, and explored further in SI 6.2, will be UHV. These are not affected by this sensitivity.

4.3.7 Sensitivity to solar PV expansion

To simulate the impact of increasing solar electricity capacity in China, we consider a sensitivity case for 2030 in which a solar fleet of 350 GW – 14, 201, 37 and 98 GW in NE, NW, S and SH, respectively – is added, the higher end of projections extrapolating from 2020 based on 20 GW annual installations[***]. We construct solar generation profiles using a typical solar generation curve for a PV plant at 36.25N 120.75W in California[29], which has a relatively high capacity factor of 18%. This profile

is scaled to local solar time for each region to account for the fact that China does not have different time zones for western and eastern regions. Hence, we add one hour for NE and SH, do not change S, and subtract two hours for NW.

We subtract this generation (0.55 PWh in total) from demand to generate new net load curves which are used as inputs to the wind selection method. We find that this results in a reduction in reference wind potential of 0.38 PWh to 2.21 PWh. Importantly, this approach gives solar priority access to the grid; hence, all coincident curtailment is attributable to wind. In fact, the results show that additional solar generation results in roughly 70% of equivalent curtailment, reflecting the fact that at high wind penetrations there is significant curtailed wind generation during hours of solar generation. This is fairly robust to different LCOE thresholds (see Table S12). Our sensitivity case cannot fully capture the impact of a given level of solar generation on wind curtailment, because in reality, solar will be subject to curtailment as well, in ways that influence the economics of grid-integrated wind.

Table S12. Wind potential and increased curtailment resulting from solar generation for various cost thresholds.

LCOE Threshold (yuan/kWh)	Solar Generation (PWh)	Wind Potential (PWh)	Increased Curtailment (PWh)
0.5	0.55	1.65	0.38
0.6	0.55	2.21	0.38
0.7	0.55	2.43	0.42

4.3.8 Sensitivity to demand growth projections

In terms of demand forecasts, the central case used in the paper is 9.9 PWh in 2030, taken from the mean of low and high demand scenarios in [6]. This works out to annual growth rates over 2011-2015, 2016-2020 and 2021-2030 periods of 8%, 5.2% and 2.2%, respectively. We consider here low and high demand scenarios of 9 PWh and 11 PWh, respectively. Wind potential and share of the total generation mix are shown in Table S13. Importantly, the share of integrated wind does not change substantially as total electricity demand changes.

Table S13. Wind potential and wind penetration for various demand scenarios.

Demand scenario	Electricity demand	Integrated wind	Wind penetration
Low	9 PWh	2.43 PWh	27.0%
Base	9.9 PWh	2.59 PWh	26.2%
High	11 PWh	2.81 PWh	25.5%

5. Full results

Table S14. All sensitivities for physical and economic wind potential.

Parameter Estimation	**Total Potential (PWh)**		
Sensitivity:	*Base*	*Low*	*High*
Physical Spacing			
Onshore: 2.58 MW/km^2 (1.5, 4.5)	22.5	13.1	39.5
Offshore: 5 MW/km^2 (4.5, 5.6)	3.9	3.5	4.3
Total	26.4	16.6	43.7
Water Depth			
Offshore: 50 m (20, 100)	3.9	1.5	5.6
Total	26.4	24.0	28.1
Economic			
LCOE threshold: 0.60 yuan/kWh (0.50, 0.70)			
Onshore	16.8	12.1	19.6
Offshore	1.0	0.5	2.0
Total	17.8	12.6	21.6
Capital cost			
Onshore: 7000 yuan/kW (8000, 6000)	16.8	13.9	19.5
Offshore: 13,000 yuan/kW (16000, 10000)	1.0	0.5	2.2
Total	17.8	14.4	21.7
O&M cost: 100 yuan/MWh (150, 50)			
Onshore	16.8	14.6	18.4
Offshore	1.0	0.6	1.5
Total	17.8	15.2	19.9

Table S15. All sensitivities for grid-integrated wind potential.

Parameter Estimation	**Total Potential (PWh)**		
Sensitivity:	*Base*	*Low*	*High*
Grid			
Sample LCOE thresholds: 0.60 yuan/kWh (0.50, 0.70)			
Onshore	2.22	1.87	2.44
Offshore	0.37	0.16	0.41
Total	2.59	2.03	2.85
Spacing			
Onshore: 2.58 MW/km^2 (1.5, 4.5)	2.22	2.12	2.42
Offshore: 5 MW/km^2 (4.5, 5.6)	0.37	0.39	0.23
Total	2.59	2.51	2.65
Capital cost			
Onshore: 7000 yuan/kW (8000, 6000)	2.22	2.12	2.36
Offshore: 13,000 yuan/kW (16000, 10000)	0.37	0.12	0.51
Total	2.59	2.24	2.87
O&M cost: 100 yuan/MWh (150, 50)			
Onshore	2.22	2.04	2.42
Offshore	0.37	0.25	0.40
Total	2.59	2.29	2.82
Integration cost *(see Supplementary Materials 3)*			
Onshore	2.22	2.22	2.24
Offshore	0.37	0.37	0.37
Total	2.59	2.59	2.61
UHV cost *(see Supplementary Materials 3)*			
Onshore	2.22	2.13	2.25
Offshore	0.37	0.38	0.37
Total	2.59	2.51	2.62
Coal flexibility *(see Supplementary Materials 3)*			
Onshore	2.22	1.86	2.62
Offshore	0.37	0.20	0.43
Total	2.59	2.07	3.05

6. Model Validation

6.1. Model estimation of curtailment

We validated our choice of the range of must-run threshold model parameters, key determinants of curtailment, by comparing to historical curtailment in two relatively isolated systems, Northeast (NE) and Jilin, a province within NE. We cannot expect to

recreate precisely historical levels of curtailment because of simplifications made in the dispatch model to make the combined expansion-dispatch problem tractable. This trade-off is common in complex power systems models capturing decisions over multiple time horizons. In our formulation, these include intra-regional bottlenecks as well as regulatory factors in China influencing operation of coal plants and interconnections that are difficult to capture. Regulatory factors, in particular, are potentially very significant in explaining current high curtailment rates[8]. Importantly, our modeled sensitivity ranges capture observed curtailment in the single province Jilin, and underpredict curtailment in the whole region. The sensitivity results further lend strength to the claim that flexibility of coal generation is an important determinant of grid-integrated wind potential.

The Northeast Grid has significant curtailment challenges and relatively small interchanges with other grid regions (21.4 TWh in 2014, accounting for 5% of regional consumption), making it an ideal case for comparison. In 2013, the Northeast Grid—consisting of Heilongjiang, Jilin, Liaoning and Eastern Inner Mongolia—reported curtailments of 6.6 TWh, or 15.5%. Jilin typically has the highest curtailment rates in the region, reaching 1.6 TWh, or 22% in 2013[30].

Since curtailment within a region in our model (excluding inter-regional transmission) is driven solely by the size of the base layer, we compare parameters used to characterize this layer with those implied by historic curtailment levels. Namely, we consider two flexibility parameters related to coal power -- minimum loading of electricity-only plants (ML_{std}) and CHP (ML_{CHP})— and one related to hydropower. While Jilin had a relatively large hydropower capacity in 2013 (4.4 GW), most of these plants are dispatched by the regional operator for inter-seasonal balancing, leaving only 195 MW dispatched by the provincial grid[31]. This leads to different operations, and for this case (*LocalHydro*) we reduce the amount of hydro that can be relied on to meet local peak load. If the fraction of local hydro available to meet daily peak loads were increased to 700 MW, curtailment reduces by roughly 3 percentage points. (For the entire NE region validation, we assume full access to hydropower resources.)

The main results of the comparison are reported in Table S16 below. We find that our modeled sensitivity ranges capture observed curtailment in Jilin, even after allowing for exports. Those same parameters underpredict curtailment in the NE region, which we

attribute to intra-regional barriers to trade and regulatory bottlenecks. Since the focus of our analysis is the year 2030, after the current round of electricity reforms aimed at improving inter-provincial trading is expected to be completed and following continued massive transmission build-outs[6], we argue that our modeling simplification is instructive. We address the cost implications of this inter-provincial transmission assumption under the transmission cost section (SI 3.2.4) and estimated SH intra-regional transmission requirements in SI Section 6.2.

Table S16. Actual and modeled curtailment in Jilin, Jilin (300MW constant exports), and Northeast for various flexibility scenarios

	Actual		**Modeled**							
Coal Flexibility Scenarios			CoalFlex						Base Case	
			ML_{std} =60% CHP fixed *LocalHydro*		ML_{std}=60% CHP fixed		ML_{std}=60%		ML_{std}=50%	
	%	TWh	%	TWh	%	TWh	%	TWh	%	TWh
Jilin	22.0	1.6	40.5	3.4	21.3	1.8	5.2	0.4	2.8	0.2
+ *Export*			33.2	2.8	16.7	1.4	3.0	0.3	1.6	0.1
Northeast	15.5	6.6			5.6	2.8	1.4	0.7	0.2	0.08

Next, we explain how we parameterized the validated systems. For both validations, we use 2013 data—demand using the same construction method above, wind profiles, and capacities[27,30]. We construct an aggregate wind profile for each province by averaging the estimated power outputs over all MERRA cells contained within a province (fractions of cells included). Not considering precise siting of wind farms introduces some bias in our estimates: our annual capacity factors are roughly 15% larger than historic generation after accounting for reported curtailment. As the purpose of our analysis to 2030 is to find total wind potential, and not to consider existing (perhaps inefficiently sited) installations, we use these profiles and compare both total and percentage share of curtailment. These are scaled to approximate mid-2013 capacities to account for grid connections completed within the year. Wind curtailment is then estimated from the dispatch model as a function of the base layer parameters.

Jilin has some export linkages with neighboring Liaoning, but despite the excess supply associated with wind and high cogeneration capacity, total exported generation was only 5% in 2011 (imports are negligible), or roughly 300MW average exports to Liaoning. We test this effect, assuming constant flow, and find some reductions in modeled curtailment (see Table S16).

6.2. Intra-regional transmission constraints

We estimate intra-regional transmission interconnections in SH necessary to achieve wind potentials at the levels determined using the aggregate model neglecting such constraints. We proceed by constructing generation capacities, demand profiles and modeled wind profiles integrated into the three regional grid jurisdictions within SH (North China Grid inclusive of West Inner Mongolia, East China Grid, and Central China Grid). We find that only the North China Grid (NCG) has significant integration challenges requiring balancing across jurisdictions. We then evaluate curtailment under our reference case varying export transmission capacities from NCG to the two other SH jurisdictions. Given the majority of SH curtailment is expected to occur in NCG, we find that interconnection capacities with neighboring ECG and CCG of 130-150 GW are necessary to achieve the aggregate levels. This level of interconnection is realistic based on current plans by State Grid. This level of wind transmission would result in utilization rates of transmission lines from avoided curtailed wind alone of 35-40%, most of the typical transmission expansion design criterion in China of 45% line loading.

The details of each step are as follows:

(1) Calculate wind totals in each disaggregated grid region

We divide SH according to current regional grid jurisdictions (plus West Inner Mongolia) into three regions: North China Grid (NCG; Beijing, Tianjin, Hebei, Shanxi, Shandong, West Inner Mongolia), East China Grid (ECG; Shanghai, Jiangsu, Zhejiang, Anhui, Fujian) and Central China Grid (CCG; Henan, Hubei, Hunan, Jiangxi, Chongqing, Sichuan). The remaining regions—NE, NW and S—are left the same. We calculate wind totals by generated region (ignoring inter-regional transmission), finding that the majority of SH wind is located in NCG, shown in Table S17.

Table S17. Wind generation in six-region disaggregation in *Reference*.

	NE	NW	S	NCG	ECG	CCG
Fraction of Total Wind Generation	14.1%	21.0%	13.8%	40.6%	8.4%	2.1%

We next allocate wind integrated into three SH grid jurisdictions from the two UHV pathways, counting all NE→SH in the closest SH jurisdiction, NCG, and splitting NW→SH between ECG and CCG. In terms of the ratio of wind to total electricity demand, NCG has the highest ratio within SH as in Table S18.

Table S18. Wind generation as share of demand in six-region disaggregation after main inter-region UHV transmission, *prior* to SH intra-regional integration in *Reference*.

	NE	NW	S	NCG	ECG	CCG
Wind Penetration (Pre-intra-SH integration)	19.8%	31.1%	22.5%	52.6%	13.4%	9.3%

(2) Calculate NCG curtailment at various intra-SH interconnection levels

Focusing on the role of NCG, we calculate 2030 forecasted generation layers (465 GW coal, of which 151 GW is CHP, 4 GW hydro, and 15 GW gas), with the difference in CHP capacity between NCG and SH attributable to industrial CHP loads in more southern regions[26]. Using the same dispatch validation approach as SI 6.1, we calculate curtailment below the must-run layer in NCG varying the export capacity to other regions. We argue that given the smaller fraction of integrated wind in ECG (13.4%) and CCG (9.3%), together with abundant hydro in CCG, the specifics of integration in each of these two regions will be less influential than NCG (52.6%) on the results. Wind curtailment and line utilizations arising just from avoided wind curtailment in NCG are in Figure S10.

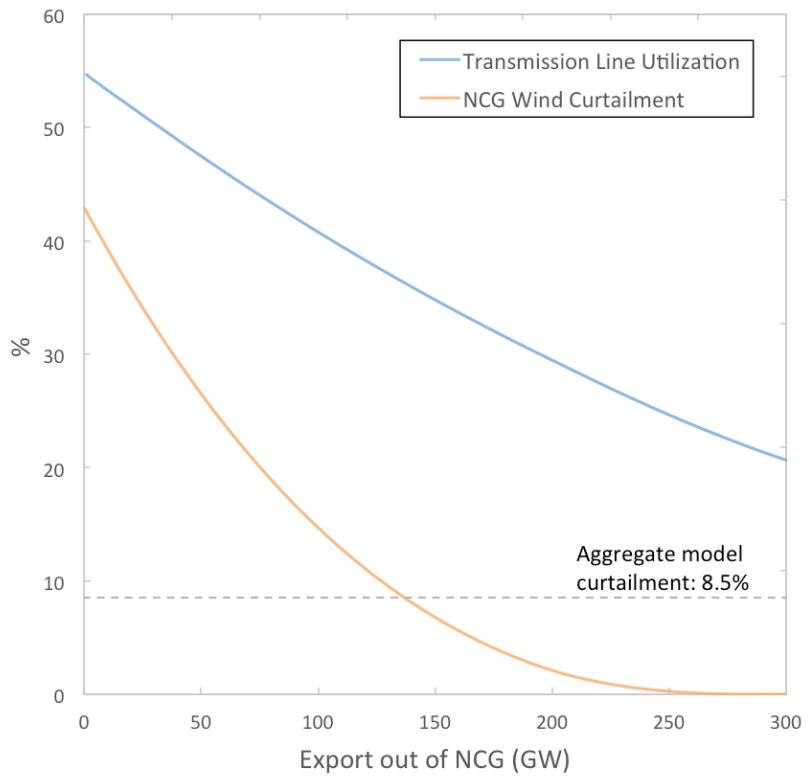

Figure S10. Wind curtailment in North China Grid (including West Inner Mongolia) for various transmission export capacities to East China Grid and Central China Grid

Attributing the aggregate model curtailment in SH entirely to NCG (an effective curtailment rate in NCG of 8.5%), we find that interconnection capacities of 130-150 GW are necessary to reduce NCG curtailment to the aggregate model levels. Beyond these levels, intra-SH transmission constraints are no longer binding, and aggregate curtailment is driven by must-run generation and meeting peak load.

While transmission plans out to 2030 are subject to considerable uncertainty, this level of interconnection is realistic given current plans by State Grid. For example, significant new interconnections are envisioned from West Inner Mongolia (in NCG) to the rest of NCG and to ECG[32]. Importantly, the modeled NCG-ECG and NCG-CCG interconnections would result in utilization rates of transmission capacity of 35-40%, achieving from avoided curtailed wind alone most of the typical transmission expansion design criterion in China of 45% line loading, with the remaining to be met by non-wind generation.

7. Calculating non-fossil energy in 2030

Our grid integration model described in Supplementary Information 3 includes detailed projections for nuclear and hydro, with capacity assumptions based on government plans[4]. Nuclear, hydro, and wind are the largest overall contributors to the non-fossil energy target—through 2030, the contribution from biomass electricity and bio-based fuels is expected to remain negligible, based on government plans. In calculating generation, nuclear is assumed to run at full capacity, and hydro at 40% (consistent with recent years). Hydropower curtailment is not allowed, assuming (1) there is sufficient storage, and (2) China's grid operators do not spill hydro. Solar generation, based on 350 GW installed, at 18% capacity factor would be a smaller contributor at 0.55 PWh. After considering curtailment including coincident curtailment with wind (described in 4.3.7), solar would be a smaller contributor at 0.17 PWh. Biomass capacity of 50 GW according to projections[6] operating at 60% capacity factor would be even smaller. The primary energy breakdown and totals we assume for 2030 are in Table S19 and consistent with published model projections in the "Accelerated Effort" scenario reported in [33].

Table S19. Nuclear and hydro capacity and generation by region assumed in the grid integration model and consistent with national plans.

Region	Nuclear (Cap, GW)	Nuclear (Gen, PWh)	Hydro (Cap,GW)	Hydro* (Gen, PWh)	Nuclear + Hydro* (Gen, PWh)
NE	14	0.12	7	0.06	0.19
NW	0	0	22	0.19	0.19
S	45	0.39	64	0.56	0.96
SH	92	0.80	119	1.04	1.85
Total	**151**	**1.32**	**213**	**1.86**	**3.18**

**assuming 40% capacity factor*

In calculating the contribution of wind to primary energy, we use the Chinese convention of average coal-fired power plant heat rates when converting electricity to

energy-equivalent, which for 2030 we assume will fall to 270 grams coal-equivalent (gce) per kWh. This is different than many international conventions, including that employed by the International Energy Agency, which converts electricity to energy based on energy content ignoring thermodynamic losses in thermal generation (i.e., 1 kWh = 3600 kJ = 123 gce). Resulting primary energy totals and percentages for the base case are in Table S20, and for coal flexibility scenarions in Table S21.

Table S20. Non-fossil generation as a share of total primary energy in 2030. Total primary energy in 2030 is estimated at 5.9 btce[33].

	Wind	**Nuclear**	**Hydro**	**Solar***	**Biomass**	**All**
Generation (PWh)	2.59	1.32	1.86	0.17	0.26	6.20
Primary energy (btce)	0.70	0.36	0.50	0.05	0.07	1.68
% Primary energy	11.9%	6.0%	8.5%	0.8%	1.2%	28.4%

*Solar incorporates all wind-solar coincident curtailment.

Table S21. Effect of coal flexibility on wind generation as a share of total primary energy in 2030. Total primary energy in 2030 is estimated at 5.9 btce.

	CoalFlex	***Reference***	***CoalRigid***
Generation (PWh)	3.05	2.59	2.07
Primary energy (btce)	0.82	0.70	0.56
% Primary energy	14.0%	11.9%	9.5%

8. Supply curve comparison

We compare our supply curve to that generated by a leading assessment[34], superimposing our results for grid-integrated economic potential (orange curve) on previous estimates (black curve) of economic potential (not including grid integration costs), as shown in the Figure S11. Our central estimate and range for economic potential under LCOEs between 0.5 and 0.7 yuan/kWh contains that from the literature. Differences in the shapes of the two curves for economic potential are likely due to

variation in the wind resource data sets, turbine spacing, land availability, and turbine cost assumptions.

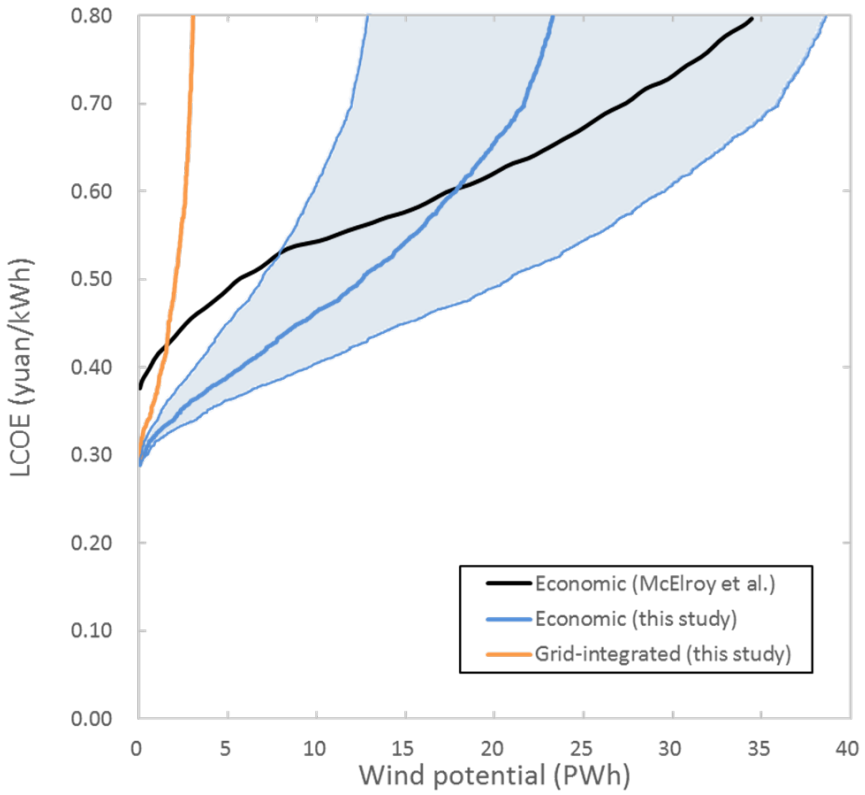

Figure S11. Comparison between the economic and grid-integrated supply curves of this study and [34].

References:

1. Hong, L. & Moller, B. Offshore wind energy potential in China: Under technical, spatial and economic constraints. *Energy* **36**, 4482–4491 (2011).

2. Hirth, B. D. & Schroeder, J. L. Documenting wind speed and power deficits behind a utility-scale wind turbine. *J. Appl. Meteorol. Climatol*. **52**, 39–46 (2013).

3. State Administration of Taxation. Notice of the State Administration of Taxation on Prepayment of Enterprise Income Tax [No. 17]. (2008).

4. Holttinen, H. et al. Impacts of large amounts of wind power on design and operation of power systems, results of IEA collaboration. *Wind Energy* **14**, 179–192 (2011).

5. CSER (China Society of Economy Reform). Compensation Mechanisms for Ancillary Services for Grid Integration of Large-scale Renewables. (2012).

6. Zhang, Y., Bai, J. & Cheng, L. *Non-fossil Energy Development Objective and Realizing Route in China.* (China Electric Power Press, 2013).

7. NEA (National Energy Administration), Northwest China Energy Regulatory Bureau. Pilot Measures for Northwest Grid Reserve Capacity Regulation. Retrieved from http://xbj.nea.gov.cn/xxgk/content_19_81_86_0_4416.html. (2012).

8. Zhao, X., Zhang, S., Zou, Y., & Yao, J. To what extent does wind power deployment affect vested interests? A case study of the Northeast China Grid. *Energy Policy* **63**, 814–822 (2013).

9. NDRC (National Development and Reform Commission) & NEA (National Energy Administration). *Guiding Opinion Regarding Improving Electricity System Operational Adjustments for Increased and Complete Clean Energy Generation* (No. 518). (2015).

10. NBS (National Bureau of Statistics). Monthly Electricity Production (various years). Accessed from the CEIC Database. (2015).

11. DERC (Draworld Environment Research Center). *Provincial hourly load curve for summer and winter typical days in 2010*. Internal report. (2015).

12. Southern Grid. *Hourly load curve of Guangdong Province in 2010*. Internal report. (2012).

13. SERC (State Electricity Regulatory Commission). Total Daily Electricity Data by Province. Accessed from the CEIC Database. (2016).

14. Kumar, N., Besuner, P., Lefton, S., Agan, D., & Hilleman, D. Power Plant Cycling Costs (pp. 275–3000). Golden, CO: National Renewable Energy Laboratory. Retrieved from http://www.nrel.gov/docs/fy12osti/55433.pdf. (2012).

15. Wu, J., Wang, J., & He B. Analysis and Suggestion on Technical and Economic Feasibility of UHVDC Project Construction for Wind Power Transmission. *Wind Energy* **10** (in Chinese). (2013).

16. Sun, K. Economic Analysis on UHV Half-wavelength AC Power Transmission. *Power System Technology* **9** (in Chinese). (2011).

17. Cai, R., Yue, C., & Xie, H. The Economic Feasibility of Transmission On-shore Large Scale Wind Power by Classical HVDC. *Southern Power System Technology,* **7**(6), 13-18. (in Chinese). (2013).

18. Huang, Y., Wang, Z., Liu, J., & Li J. Economic Analysis of Wind Power by UHV DC Transmission. *Electric Power Construction*. **32**(5), 100-103. (in Chinese). (2011).

19. ERI (Energy Research Institute). *China Wind Energy Roadmap 2050*. (2014).

20. Bozzuto, C. (Ed.). *Clean Combustion Technologies* (5th ed.). Windsor, CT: Alstom. (2009).

21. Davidson, M., Li, C.-T., Karplus, V. (2015). Grid Operations and Renewable Energy Integration in China. Mimeo (based on interviews conducted in China's Northwest and Inner Mongolia), forthcoming as a Working Paper in Spring 2016.

22. Ding, H., Hu, Z., & Song, Y. Stochastic optimization of the daily operation of wind farm and pumped-hydro-storage plant. *Renewable Energy*, **48**, 571-578. (2012).

23. Zhang, N., Lu, X., McElroy, M. B., Nielsen, C. P., Chen, X., Deng, Y., & Kang, C. Reducing curtailment of wind electricity in China by employing electric boilers for heat and pumped hydro for energy storage. *Applied Energy*. (in press).

24. Dong, J., Xue, G., & Li, R. Demand response in China: Regulations, pilot projects and recommendations - A review. *Renewable and Sustainable Energy Reviews*, **59**, 13-27. (2016).

25. Liu, Y., Eyre, N., Darby, S., Keay, M., Robinson, M., & Li, X. *Assessment of Demand Response Market Potential and Benefits in Shanghai*. Environmental Change Institute & Oxford Institute for Energy Studies. Retrieved from http://www.nrdc.cn/phpcms/userfiles/download/201509/01/Assessment%20of%20Demand%20Response%20Market%20Potential%20and%20Benefits%20in%20Shanghai.pdf. (2015).

26. Xiong, W., Wang, Y., Mathiesen, B. V., Lund, H., & Zhang, X. Heat roadmap China: New heat strategy to reduce energy consumption towards 2030. *Energy*, **81**, 274-285. (2015).

27. CEC (China Electricity Council). Electricity industry statistics summary 2012. Internal report. (2013).

28. THUBERC (Tsinghua University Building Energy Research Center). *2015 Annual Report on China Building Energy Efficiency*. China Architecture & Building Press. (2015).

29. NREL (National Renewable Energy Laboratory). Solar Power Data for Integration Studies. DOE/NREL/ALLIANCE. http://www.nrel.gov/electricity/transmission/solar_integration_methodology.html . Accessed February 11, 2016. (2016).

30. NEA (National Energy Administration). *2013 Status of the Wind Industry*. National Energy Administration. Retrieved from http://www.cnrec.org.cn/hd/2014-02-25-412.html. (2014).

31. Jilin Grid Company. Electricity Market Exchange Information Annual Report 2012. (2013).

32. Han, F., Song, F., Luo, J., Lu, C. Focuses on development of transmission grid in the 13th Five-Year Plan. *Electric Power* **1** (in Chinese). (2015)

33. Zhang, X., Karplus, V. J., Qi, T., Zhang, D. & He, J. Carbon emissions in China: How far can new efforts bend the curve? *Energy Economics*, **54**, 388–395. (2016).

34. McElroy, M. B., Lu, X., Nielsen, C. P. & Wang, Y. X. Potential for wind-generated electricity in China. *Science* 325, 1378–1380. (2009).

---

[*] Source: Xinhuanet.cn. Inner *damaoqi* million-kilowatt wind power base construction plan approved (In Chinese: 内蒙古达茂旗百万千瓦级风电基地建设规划获批) (2008). (http://news.xinhuanet.com/fortune/2008-10/18/content_10214752.htm).

[†] Source: Dianlan.cn. 200,000 kilowatts of Huaneng wind power projects approved. (In Chinese: 华能 20 万千瓦风电项目获批准) (2013). (http://kuaibao.dianlan.cn/cont-54330.html).

[‡] Source: Zhangjiakou Development and Reform Commission. 300,000 kilowatts of wind power projects in Hebei Development and Reform Commission to obtain approval. (In Chinese: 康保五福堂 30 万千瓦风电项目取得河北发改委核准批复) (2013). (http://www.zjkfgw.gov.cn/Project/ShowArticle.asp?ArticleID=2745).

[§] Source: Kailu.gov.cn. Wind Farm Construction Progress. (In Chinese: 风电场建设进展情况) (http://kailu.gov.cn/kldzxxw/zw.aspx?wzid=677). Note: Data for Beiqinghe to Jianhua_No.2.

[#] Source: (In Chinese: 内蒙古自治区环境保护厅关于 2014 年 6 月 11 日拟作出的建设项目竣工环境保护验收意见的公示) (2014). (http://www.nmgepb.gov.cn/web/ywgs/ys_4724/201410/t20141013_1466414.html).

[‖] Source: Business.sohu.com. China's largest single wind farm grid run successfully in Fuxin, Liaoning Province. (2009). (In Chinese: 中国最大单个风电场在辽宁阜新成功并网运行).

[**] Source: Energy.people.com.cn. Baotou City Planning 18 million kilowatts of wind power generation. (In Chinese: 包头市规划 1800 万千瓦风电发电 或可打捆外送). (2012). (http://energy.people.com.cn/n/2012/1025/c71890-19388024.html).

[††] Source: zj.sina.com.cn. Zhejiang Province's first offshore wind farm approved. (In Chinese: 浙江省首个海上风电场获批). (2013). (http://zj.sina.com.cn/news/d/2013-12-28/0758155596.html).

[‡‡] Source: Fujian.gov.cn. Large offshore wind farm to be built. (In Chinese: 大练将建海上风电场). (2013). (http://www.fujian.gov.cn/zwgk/zfgzdt/sxdt/ptzhsyq/201311/t20131105_673892.htm).

[§§] Source: Jiaxing News. Jiaxing the 2nd offshore wind farm projects to carry out wind measurement. (In Chinese: 嘉兴 2 号海上风电场项目获准开展测风工作). (2012). (http://cnjxol.com/xwzx/jxxw/szxw/content/2012-03/09/content_1948842.htm)

[***] Source: Xinhua. China's PV power capacity to hit 150 gigawatts by 2020. (2015). (http://news.xinhuanet.com/english/2015-10/13/c_134710495.htm)